

Phase structures and electrical properties of $(1-x)(\text{K}_{0.48}\text{Na}_{0.52})\text{NbO}_3-x(\text{Ba}_{0.85}\text{Ca}_{0.15})(\text{Zr}_{0.1}\text{Ti}_{0.9})\text{O}_3$ lead-free ceramics

Jigong Hao, Wei Li, Wangfeng Bai, Bo Shen, Jiwei Zhai*

Functional Materials Research Laboratory, Tongji University, 1239 Siping Road, Shanghai 200092, China

Available online 17 October 2012

Abstract

Lead-free ceramics $(1-x)(\text{K}_{0.48}\text{Na}_{0.52})\text{NbO}_3-x(\text{Ba}_{0.85}\text{Ca}_{0.15})(\text{Zr}_{0.1}\text{Ti}_{0.9})\text{O}_3$ doped with 1.0 mol% MnO_2 were prepared using a solid-state reaction technique. The phase transition behavior and electrical properties of the ceramics were studied. Results show that $(\text{Ba}_{0.85}\text{Ca}_{0.15})(\text{Zr}_{0.1}\text{Ti}_{0.9})\text{O}_3$ diffuses into $(\text{K}_{0.48}\text{Na}_{0.52})\text{NbO}_3$ to form a new solid solution, and induces a phase structure transition from orthorhombic to tetragonal phase with the increase of x . At $0.04 \leq x \leq 0.06$, coexistence of the orthorhombic and tetragonal phases is observed, and enhanced piezoelectric properties are achieved in this region due to the polymorphic phase transition near room temperature. The doping of MnO_2 effectively promotes the densification of the ceramics and further enhances the piezoelectric and dielectric properties at room temperature. The ceramics with $0.04 \leq x \leq 0.06$ and 1.0 mol% MnO_2 possess excellent electrical properties: $d_{33}^* = 200\text{--}262$ pm/V, $d_{33} = 153\text{--}182$ pC/N, $\epsilon_r = 763\text{--}976$, $\tan \delta = 0.054\text{--}0.060$, $T_c = 268\text{--}312$ °C. Moreover, samples with single tetragonal phase at $x = 0.07$ have a good temperature stability in the temperature range of 25–150 °C due to the shift of the orthorhombic to tetragonal polymorphic phase transition below room temperature.

© 2012 Elsevier Ltd and Techna Group S.r.l. All rights reserved.

Keywords: A. Sintering; B. Grain size; C. Electrical properties

1. Introduction

Environmental concerns over piezoelectric ceramics motivate the development of high-performance lead-free piezoelectrics [1–3], and considerable attention for lead-free piezoelectric materials has been given to $(\text{K}_{0.5}\text{Na}_{0.5})\text{NbO}_3$ (KNN)-based ceramics since Saito et al. [1] made a breakthrough in the textured (Li, Ta, Sb)-modified KNN ceramics. For pure KNN ceramics, difficulty in sintering of the ceramics and control of stoichiometry always leads to deviation from excellent properties, and the KNN ceramics prepared using normal sintering exhibit poor piezoelectric properties [4]. To improve the densification and piezoelectric properties of KNN ceramics, many studies have been devoted to the property improvement by chemical modification [5–9], and these include the formation of solid solutions of KNN with other ABO_3 perovskites [6,7].

$(\text{Ba}_{0.85}\text{Ca}_{0.15})(\text{Zr}_{0.1}\text{Ti}_{0.9})\text{O}_3$ ceramic is a perovskite ferroelectric exhibiting a surprisingly high piezoelectric

coefficient $d_{33} = 620$ pC/N [3]. It would be advantageous to the improvement of the piezoelectric properties of KNN-based ceramics by shifting the polymorphic phase transition (PPT) to near room temperature and thus achieving a coexisted crystal structure with both orthorhombic and tetragonal phases.

In this paper, we report the preparation of a solid solution $(1-x)(\text{K}_{0.48}\text{Na}_{0.52})\text{NbO}_3-x(\text{Ba}_{0.85}\text{Ca}_{0.15})(\text{Zr}_{0.1}\text{Ti}_{0.9})\text{O}_3(\text{KNN}-x\text{BCZT})$ doped with 1.0 mol% MnO_2 by the conventional sintering method. The phase structure, microstructure, electrical properties and temperature stability of KNN- x BCZT ceramics was investigated.

2. Experimental procedures

To prepare the KNN- x BCZT ceramics, KNN and BCZT powders were first synthesized at 850 °C for 5 h and 1200 °C for 4 h, respectively, by a solid state reaction. After the calcination, KNN, BCZT, and MnO_2 powders were weighted according to the formulas and then ball milled for 24 h. The resulting powders were mixed with a

*Corresponding author. Tel.: +86 21 65980544; fax: +86 21 65985179.
E-mail address: apzhai@tongji.edu.cn (J. Zhai).

polyvinyl alcohol binder solution and then pressed into disk compacts. The disk compacts were sintered at 1120–1160 °C for 3 h in air.

Phase structure of the ceramics was identified by using X-ray diffraction (XRD, Bruker D8 Advanced, with Cu K α radiation). The surface morphology of the ceramics was observed by scanning electron microscope (SEM, JSM-5510LV, Japan). For the electric measurements silver paste was coated on both sides of the sintered samples and fired at 600 °C for 10 min to form electrodes. Dielectric properties were measured using an HP 4284A precision LCR meter (Agilent, Palo Alto, CA). The electric-field-induced polarization (P – E) and strain (S – E) measurements were carried out using a ferroelectric test system (PrecisionPremier II, USA) connected with a miniature plane-mirror interferometer and the accessory laser interferometer vibrometer (SP-S 120/500, Germany). The piezoelectric constant d_{33} of poled samples was measured using a quasi-static d_{33} meter (ZJ-6A). The planar electromechanical coupling factor k_p was calculated following IEEE standards by using an impedance analyzer (HP 4294A).

3. Results and discussion

Fig. 1 shows the XRD patterns of the KNN– x BCZT–Mn ceramics. All the ceramics possess a pure perovskite structure without any secondary phases, suggesting that BCZT and MnO₂ have diffused into the KNN lattices to form a homogeneous solid solution. Ceramics with $x < 0.04$ possess an orthorhombic structure with the splitting of the (100)/(010) and (200)/(020) characteristic peaks. As x increases, a tetragonal phase appears and increases continuously in volume. At $x = 0.07$, the ceramic possesses single tetragonal phase as shown the change of the above characteristic peak s [7,9]. Accordingly, coexistence of the orthorhombic and tetragonal phases is obtained at $0.04 \leq x \leq 0.06$ in the present study.

Fig. 2 shows SEM images of the KNN– x BCZT ceramics: (a) without MnO₂ and (b) with 1.0 mol% MnO₂ doping.

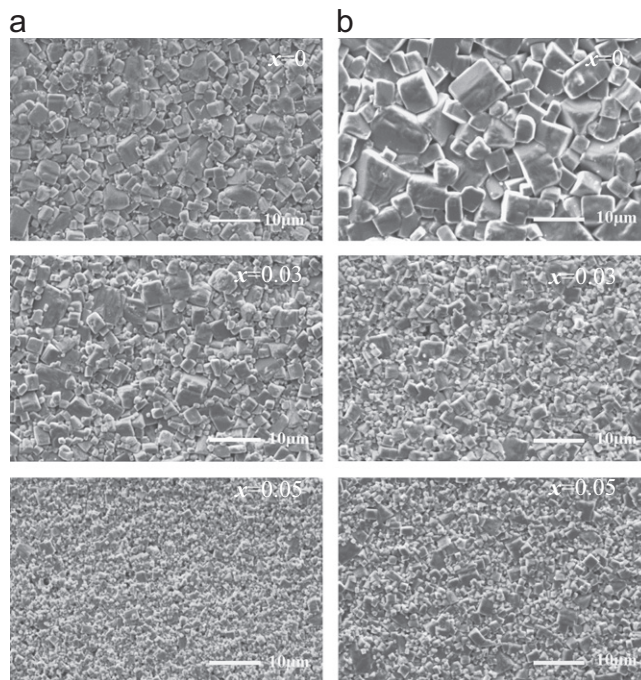


Fig. 2. SEM images of the KNN– x BCZT ceramics: (a) without MnO₂ doping and (b) with 1.0 mol% MnO₂ doping.

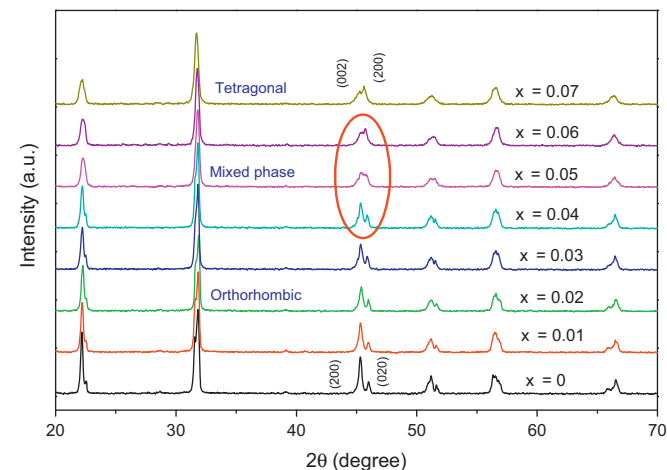


Fig. 1. XRD patterns of the KNN– x BCZT–Mn ceramics as a function of x .

It can be clearly observed that after BCZT doping in KNN ceramics, the grains became distinctly smaller and more uniform. This reveals that a small amount of BCZT doped in KNN ceramic, as a grain growth inhibitor, has an evident effect on grain size reduction. The results are well accorded with the previous results that the introduced second component with ABO₃ perovskites in KNN-based ceramics usually act as grain growth inhibitor [9]. In addition, it is observed that the ceramics at high BCZT content without MnO₂ addition become porous, suggesting that excess BCZT doping degrades the sintering performance of the ceramics, and thus results in the significant decrease in densification. While after adding 1.0 mol% MnO₂, all the ceramics can be well sintered at a lower temperature and have a dense structure with a high relatively density $> 96\%$.

Fig. 3(a and b) shows temperature dependence of the dielectric constant ϵ_r for KNN– x BCZT ceramics without MnO₂ and with 1.0 mol% MnO₂ doping, respectively. Meanwhile variations of the phase transition temperatures, and room temperature dielectric constant ϵ_r and loss $\tan \delta$ with x are presented in Fig. 3(c and d). It can be found that KNN ceramic exhibits the classic ferroelectric characteristics, undergoing the orthorhombic–tetragonal phase transition at 200 °C (T_{O-T}) the tetragonal–cubic phase transition at 406 °C (T_c). After the addition of BCZT, the ceramics display similar temperature dependences of ϵ_r , but with the two transition peaks shifted to lower temperatures as clearly show in Fig. 3(c). The result is in conformity with the previous results that the introduced second component MTiO₃ in KNN-based ceramics usually decreases both T_{O-T} and T_c [6,7,9,10], which are mainly

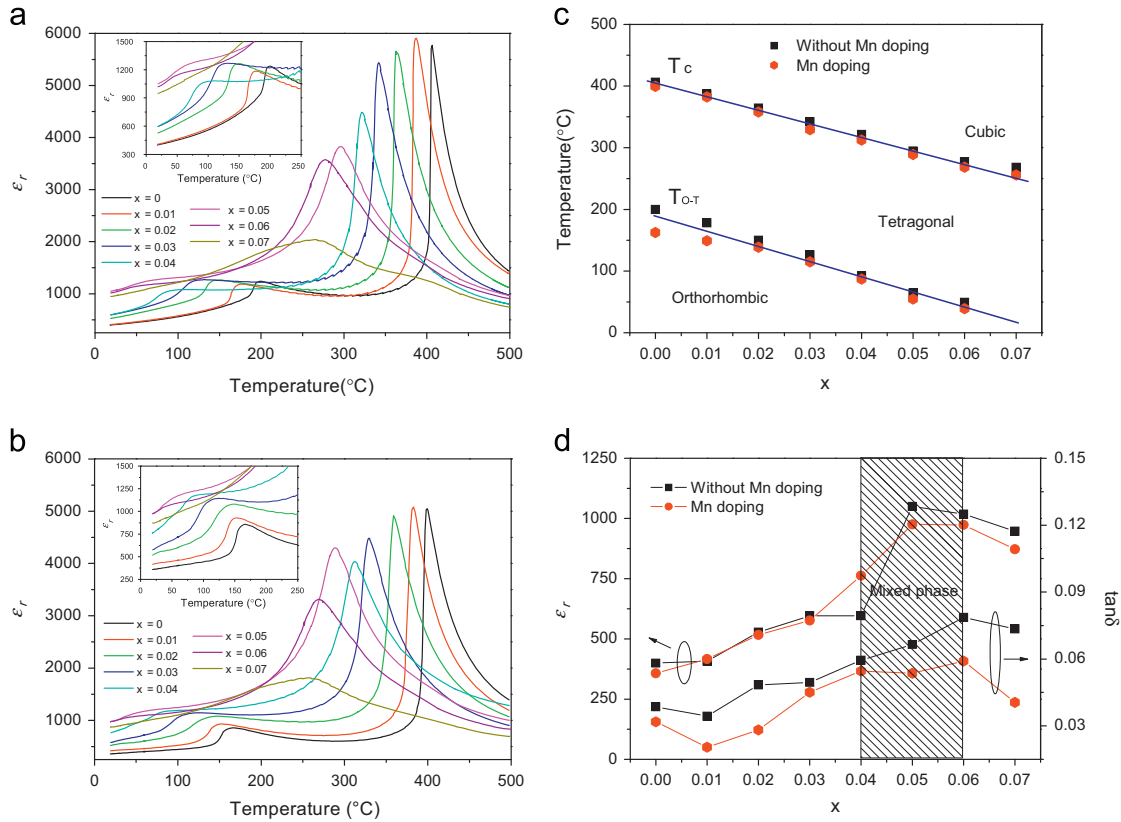


Fig. 3. Temperature dependence of the dielectric constant for KNN-*x*BCZT ceramics measured at 10 kHz: (a) without MnO₂ and (b) with 1.0 mol% MnO₂ doping, (c) *T_c* and *T_{O-T}*, and (d) *ε_r* and tan *δ* (RT) of the ceramics as a function of *x*.

affected by the A-site cations and B-site cations, respectively. At *x*=0.07, only the cubic–tetragonal phase transition is observed above room temperature which means that the structure has changed from orthorhombic to tetragonal. The observed *T_{O-T}* for the ceramics with 0.04 < *x* < 0.06 is close to room temperature, suggesting that the orthorhombic and tetragonal phases coexist in these ceramics, which is consistent with the results of XRD (Fig. 1). In addition, variations of room temperature *ε_r* of the ceramics with *x* as shown in Fig. 3(d) indicate that coexistence of the orthorhombic/tetragonal phases can be very helpful for the enhancement of dielectric properties.

Fig. 4 shows *P*–*E* hysteresis loops and bipolar *S*–*E* loops of KNN-*x*BCZT samples measured at 10 Hz. Samples with *x* ≤ 0.04 exhibit a well-saturated *P*–*E* hysteresis with large remnant polarizations and typical “butterfly” shaped *S*–*E* loops. However, ceramics at high BCZT content without MnO₂ dopant have poor sintering performance with porous microstructure and large electrically conductivity, no typical *P*–*E* loops and “butterfly” shape in *S*–*E* characteristics were obtained in the present study because of the contribution of electric conductivity while no apparent contribution from domain switching [11]. After doping 1.0 mol% MnO₂ in KNN-*x*BCZT, typical hysteresis loops with good square shape and “butterfly” shaped *S*–*E* characteristics were obtained in the whole compositions of *x*=0–0.07, confirming the densification effect of

MnO₂. The addition of MnO₂ weakens the ferroelectricity of the ceramics, and similar weakening effects have also been found in MnO₂ and other sintering aids modified KNN-based ceramics [12,13]. However, due to the densification effect of MnO₂, enhanced piezoelectric properties (*k_p*, *d₃₃^{*}* and *d₃₃*) are achieved in MnO₂-doped samples, which can be clearly seen in Fig. 5(a). The ceramics with 0.04 ≤ *x* ≤ 0.06 (with 1.0 mol% MnO₂) which lies on the mixed phase region possess good piezoelectric properties: *k_p*=35–39%, *d₃₃^{*}*=200–262 pm/V and *d₃₃*=153–182 pC/N, confirming the leading role of PPT for the improvement of piezoelectric properties in KNN-based ceramics. Moreover, it is noted that the values of *k_p*, *d₃₃^{*}* and *d₃₃* of samples with *x*=0.05 and 0.06 were smaller than those of *x*=0.04, although these ceramics also reside in the region of coexistence. The reduced bulk density which increases the leakage current diminishing the polarization in process should be the main reason for the decrease of piezoelectric properties. On the other hand, samples of *x*=0.05 and 0.06 are near the tetragonal side of the orthorhombic–tetragonal phase boundary, while sample of *x*=0.04 was near the orthorhombic side of the orthorhombic–tetragonal phase boundary, and thus more possible polarization is obtained there, resulting in higher piezoelectric parameters [14].

Fig. 5(b) shows temperature dependence of *P_r*, *k_p* and *d₃₃^{*}* for KNN-*x*BCZT-Mn ceramics. KNN-0.02BCZT

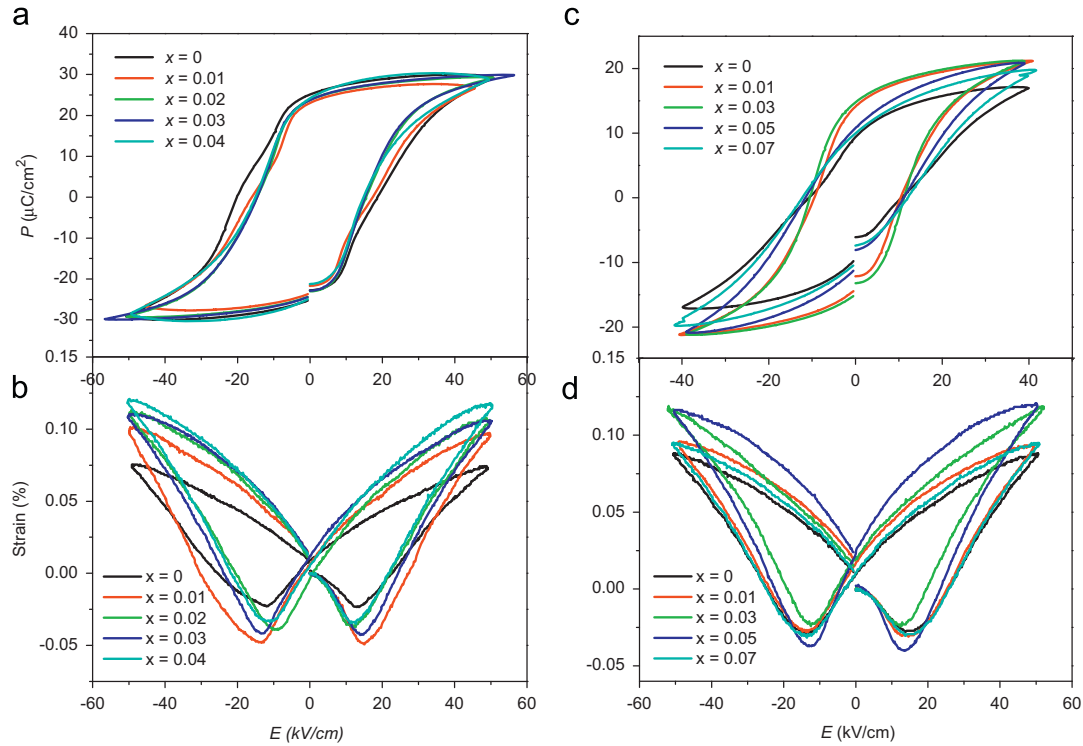


Fig. 4. P - E hysteresis loops and bipolar S - E loops of KNN- x BCZT samples measured at 10 Hz: (a,b) without MnO_2 doping and (c,d) with 1.0 mol% MnO_2 doping.

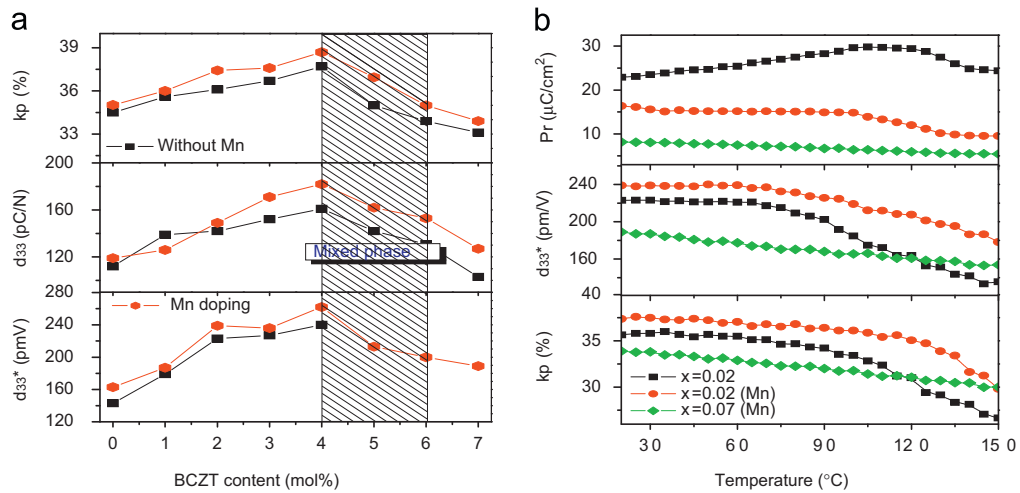


Fig. 5. (a) Compositions dependence of k_p , d_{33}^* and d_{33} and (b) temperature dependence of P_r , d_{33}^* and k_p for KNN- x BCZT-(Mn) ceramics.

samples display relatively poor temperature stability with the obvious change of P_r , k_p and d_{33}^* at the O-T phase boundary due to the appearance of PPT at around 140 °C. However, owing to the “hardening” effect of MnO_2 similar to that of CuO [15], KNN-0.02BCZT-Mn samples exhibit enhanced thermal stability at the temperature below 100 °C, where orthorhombic phase predominate. However, these values decrease fleetly across PPT, revealing that this behavior is determined by the PPT temperature, which is unaffected by “hardening” effect. Furthermore, Mn-modified KNN-0.07BCZT ceramics show the good temperature stability with a slight decrease of P_r , k_p and d_{33}^* as

temperature increases from 20 to 150 °C due to the shift of PPT below room temperature.

4. Conclusion

In this work, phase transition behavior and electrical properties of KNN- x BCZT-Mn ceramics were studied. The ceramics with $0.04 \leq x \leq 0.06$ contain both the orthorhombic and tetragonal phases at room temperature, and correspond a room temperature PPT. Owing to the more possible polarization states resulting from the coexistence of the two phases, enhanced piezoelectric properties are

obtained in this region. The doping of MnO_2 effectively promotes the densification of the ceramics and further enhances the piezoelectric and dielectric properties. The ceramics in the mixed phase region with Mn-doping possess following optimum properties: $d_{33}^* = 200\text{--}262$ pm/V, $d_{33} = 153\text{--}182$ pC/N, $\epsilon_r = 763\text{--}976$, $\tan \delta = 0.054\text{--}0.060$, $T_c = 268\text{--}312$ °C. The temperature-dependent electrical property for the $\text{KNN-}x\text{BCZT}$ system shows that thermal stability is determined by PPT temperature in KNN-based ceramics.

Acknowledgments

The authors would like to acknowledge the support from the National Natural Science Foundation of China under Grant no. 50932007.

References

- [1] Y. Saito, H. Takao, T. Tani, T. Nonoyama, K. Takatori, T. Homma, T. Nagaya, M. Nakamura, Lead-free piezoceramics, *Nature* 432 (2004) 84–87.
- [2] E. Cross, Lead-free at last, *Nature* 432 (24) (2004) 24–25.
- [3] W.F. Liu, X.B. Ren, Large piezoelectric effect in Pb-free ceramics, *Physical Review Letters* 103 (2009) 257602.
- [4] L. Egerton, D.M. Dillom, Piezoelectric and dielectric properties of ceramics in the system potassium–sodium niobate, *Journal of the American Ceramic Society* 42 (1959) 438–442.
- [5] G.Z. Zang, J.F. Wang, H.C. Chen, W.B. Su, C.M. Wang, P. Qi, B.Q. Ming, J. Du, L.M. Zheng, S. Zhang, T.R. Shrout, Perovskite $(\text{Na}_{0.5}\text{K}_{0.5})_{1-x}(\text{LiSb})_x\text{Nb}_{1-x}\text{O}_3$ lead-free piezoceramics, *Applied Physics Letters* 88 (2006) 212908.
- [6] W.J. Wu, D.Q. Xiao, J.G. Wu, J. Li, J.G. Zhu, B. Zhang, Microstructure and electrical properties of relaxor $(1-x)[(\text{K}_{0.5}\text{Na}_{0.5})_{0.95}\text{Li}_{0.05}](\text{Nb}_{0.95}\text{Sb}_{0.05})\text{O}_3-x\text{BaTiO}_3$ piezoelectric ceramics, *Ceramics International* 38 (2012) 2277–2282.
- [7] D.M. Lin, K.W. Kwok, H.W.L. Chan, Dielectric and piezoelectric properties of $(\text{K}_{0.5}\text{Na}_{0.5})\text{NbO}_3\text{--Ba}(\text{Zr}_{0.05}\text{Ti}_{0.95})\text{O}_3$ lead-free ceramics, *Applied Physics Letters* 91 (2007) 143513.
- [8] T.R. Shrout, S.J. Zhang, Lead-free piezoelectric ceramics: alternatives for PZT?, *Journal of Electroceramics* 19 (2009) 111–124.
- [9] R.Z. Zuo, X.S. Fang, C. Ye, L.T. Li, Phase transitional behavior and piezoelectric properties of lead-free $(\text{Na}_{0.5}\text{K}_{0.5})\text{NbO}_3\text{--}(\text{Bi}_{0.5}\text{K}_{0.5})\text{TiO}_3$ ceramics, *Journal of the American Ceramic Society* 90 (2007) 2424–2428.
- [10] R.P. Wang, H. Bando, M. Itoh, Universality in phase diagram of $(\text{K,Na})\text{NbO}_3\text{--MTiO}_3$ solid solutions, *Applied Physics Letters* 95 (2009) 092905.
- [11] H.X. Yan, F. Inam, G. Viola, H.P. Ning, H.T. Zhang, Q.H. Jiang, T. Zeng, Z.P. Gao, M.J. Reece, The contribution of electrical conductivity, dielectric permittivity and domain switching in ferroelectric hysteresis loops, *Journal of Advanced Dielectrics* 1 (2011) 107–118.
- [12] Q. Chen, L. Chen, Q.S. Li., X. Yue, D.Q. Xiao, J.G. Zhu, Piezoelectric properties of $\text{K}_4\text{CuNb}_8\text{O}_{23}$ modified $(\text{Na}_{0.5}\text{K}_{0.5})\text{NbO}_3$ lead-free piezoceramics, *Journal of Applied Physics* 102 (2007) 104109.
- [13] E. Li, H. Kakemoto, S. Wada, T. Tsurumi, Effects of manganese addition on piezoelectric properties of the $(\text{K,Na,Li})(\text{Nb,Ta,Sb})\text{O}_3$ lead-free ceramics, *Journal of the Ceramic Society of Japan* 115 (2007) 250–253.
- [14] J.G. Hao, R.Q. Chu, Z.J. Xu, G.Z. Zang, G.R. Li, Structure and electrical properties of (Li,Sr,Sb) -modified $\text{K}_{0.5}\text{Na}_{0.5}\text{NbO}_3$ lead-free piezoelectric ceramics, *Journal of Alloys and Compounds* 479 (2009) 376–380.
- [15] Hagh N. Marandian, K. Kerman, B. Jadidian, A. Safari, Dielectric and piezoelectric properties of Cu^{2+} -doped alkali Niobates, *Journal of the European Ceramic Society* 29 (2009) 2325–2332.